JOURNAL OF APPLIED ELECTROCHEMISTRY 11 (1981) 771–780

Evaluation of agitation within circuit board through-holes

R. HAAK, C. OGDEN, D. TENCH

Rockwell International/Microelectronics Research and Development Center, Thousand Oaks, California 91360, USA

Received 16 February 1981

A method is presented for determining the rate and uniformity of solution mass transport to the outer surfaces and within the through-holes of multilayer printed circuit boards. The method is based on the measurement of the diffusion-limited currents for a fast redox reaction at strategically located inert electrode probes. A specially fabricated test board and an electrolyte which hydrodynamically simulates the copper pyrophosphate system are described. Results are presented for a typical agitation scheme based on gas sparging and slow board motion. The method provides the basis for evaluating and improving bath agitation schemes and should be applicable to a variety of systems.

1. Introduction

Mass transport of electrolyte is a critical factor in any electroplating operation. Organic addition agents, complex metal ions and other solution species which participate in the cathodic reaction must be replenished from the solution bulk as they are reduced or included in the electrodeposit. In addition, soluble reduction products (e.g., H_2, OH^-, metal complexing agents and additive breakdown products) must be transported away from the electrode as they are generated. Efficient, uniform agitation is particularly important in circuit board plating for which organic additives, which operate under diffusion control [1], are usually used, and deposit properties are critical. For example, the dimercaptothiadiazole additives widely employed in copper pyrophosphate baths are present in concentrations of only a few parts per million but must be maintained constant at the cathode surface to attain acceptable tensile properties and uniform deposits [2, 3]. Kessler and Alkire [4, 5] and Engelmaier and Kessler [6] have shown that inadequate mass transport within through-holes also leads to poor deposits from acid copper baths, with and without organic additives. In both pyrophosphate [3, 7] and acid copper [8] systems, deposit ductility can vary by as much as a factor of five with agitation rate at a constant additive concentration. The effects of agitation on the deposit tensile strength are also significant, although less pronounced.

In spite of its importance, no reliable method has been available to measure electrolyte mass transport in most production processes, so that development of bath agitation schemes has usually been based on intuition rather than scientific method. For example, circuit board agitation schemes generally involve some combination of gas sparging and board motion, although, based on deposit uniformity†, mass transport provided by such schemes apparently varies by at least 50% over the board surfaces and considerably more within the through-holes. Consequently, circuit board quality is notoriously variable and laboratory data, even when taken under well-defined conditions, are of limited value in specifying process conditions.

In the present paper, a method is described for measuring the instantaneous rate and uniformity of mass transport provided by a given circuit board agitation scheme. With this method, an optimum agitation system, representing a compromise between a high overall rate of mass transport and minimal spatial and time variations, can be developed. Improvements might be attained with more strategically located gas spargers providing bubbles of optimum size, other patterns and rates of board

†Note that deposit uniformity provides only an indication of the agitation uniformity since thickness variations are averaged over the plating time, and other factors, such as the primary current distribution, also affect the deposit thickness.

0021–891X/81/060771–10$03.00/0

motion, electrolyte pumping through nozzles directed at the board [9], forced electrolyte flow, and ultrasonic agitation [10]. In addition, with a knowledge of the average value and variations in mass transport, the bulk bath composition and plating conditions can be specified so that critical solution species are maintained at their optimum values at the cathode surface during plating. Such mass transport optimization could also permit faster plating in some systems, providing considerable economic advantage.

2. Description of the method

In the method described here, a specially designed circuit board is immersed in an electrolyte containing the components of a fast redox couple (in a small equimolar concentration) and the current is measured at constant potential for each of a series of electrically isolated, inert electrode probes distributed along the surface and within the through-holes. Reduction (or oxidation) of one of the redox species occurs at the selected probe, whereas the reverse action occurs at the inert counter electrode so that there is no net chemical change in the system. The probe potential and redox couple concentration are chosen so that the current is diffusion limited, i.e., determined only by the rate of mass transport of reactant to the electrode surface. Comparison of the limiting currents at the isolated probes along the cathode surface, including those within the through-holes, permits the uniformity of solution mass transport provided by a particular agitation scheme to be evaluated. Since the redox reaction occurs under diffusion control, geometric factors such as the anode to cathode spacing do not affect the measurements.

An inert supporting electrolyte is employed to both lower the electrical resistance of the solution and provide the same hydrodynamic properties (kinematic viscosity and surface tension) as the plating bath of interest. A low solution resistance is desirable to facilitate control of the probe potential. The kinematic viscosity of the electrolyte is important since it determines the efficacy of agitation in producing fluid flow. The surface tension must be maintained constant to ensure that bubbles will form at the same rate and be of the same average size in the test electrolyte as in the plating bath.

It should be mentioned that the method described here does not adequately take into account natural convection which results from the solution density gradient established by depletion of metal ions in the vicinity of the cathode surface. This is because the solution density changes associated with the ferro–ferricyanide reaction, which involves two soluble species and relatively small currents, are considerably less than those associated with metal deposition. However, the contribution of natural convection to the overall mass transport rate will generally be small compared to that of the forced convection employed in most practical systems.

3. Experimental details

3.1. *Electrolyte selection*

The supporting electrolyte 1was 1.0 mol dm^{-3} KCl since this solution was found to have practically the same kinematic viscosity (0.88 centistokes compared to 0.86) and surface tension (74.58 dynes cm^{-1} compared to 75.86) at room temperature (22.5° C) as a standard copper pyrophosphate bath (22.5 g dm^{-3} Cu^{2+}, 175 g dm^{-3} $P_2O_7^{4-}$, 2.25 g dm^{-3} NH_3) at an operating temperature of 55° C. Kinematic viscosity was measured with a Cannon–Fenske viscometer [11] and surface tension was determined by the capillary rise method. Reagent-grade KCl was used in the present studies but comparable results were obtained with technical-grade material if solutions were treated with activated charcoal and filtered twice before use.

Ferro–ferricyanide was chosen as the redox couple since it is stable (in neutral and basic solutions), is generally fast and reversible, and has little tendency toward specific adsorption. The electrolyte always contained 1.0 mol dm^{-3} KCl and 3.8 mM each of $K_3Fe(CN)_6$ and $K_4Fe(CN)_6$. Typical voltammetry curves for this couple at a rotating gold disc electrode (0.32 cm^2, mounted flush with the end of a 13 mm diameter polychlorotrifluoroethylene rod by hot pressing) are shown in Fig. 1. The current plateaus were shown to be limited by mass transport; plots of the plateau current (for both the anodic and cathodic branches) versus the square root of the electrode rotation rate yield straight lines that pass through

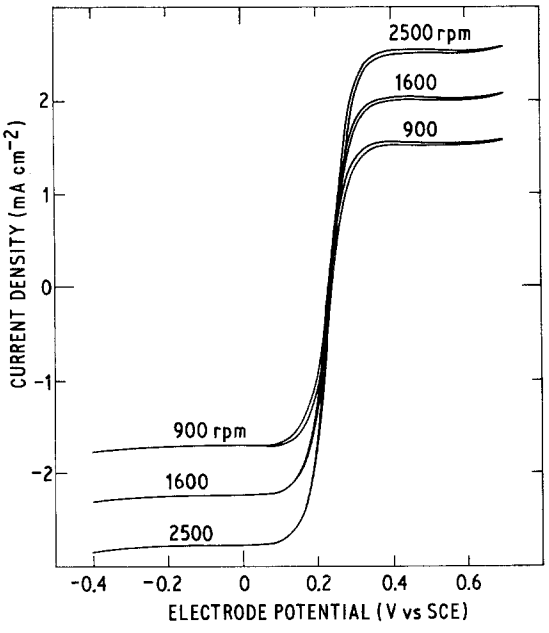

Fig. 1. Cyclic voltammograms (20 mV s^{-1}) for a Pt disc electrode at various rotation rates in a 1.0 M KCl solution containing 3.8 mM $K_3Fe(CN)_6$ and $K_4Fe(CN)_6$.

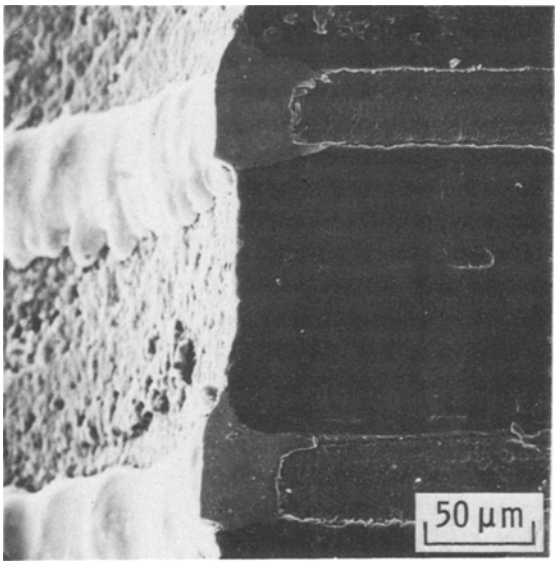

Fig. 2. Scanning electron micrograph of a cross-section of a typical gold-plated through-hole probe, showing the line of demarcation between the flush gold rings (to the left) and the underlying copper layers (to the right).

the origin [12]. The potential of probes on the test board was maintained in the diffusion-limited region potentiostatically.

3.2. *Test board fabrication*

The test board measured 23 cm x 30 cm and was constructed from five layers of 0.15 mm copper (photo-etched to form appropriate circuitry patterns) separated by 0.15 mm layers of epoxy–fibreglass laminant using standard multilayer printed circuit board manufacturing techniques. The outer board surfaces were clad with 0.9 mm epoxy-glass so that the final board thickness was 3.2 mm. The copper rings within most of the through-holes were recessed ~ 0.04 mm by chemical etching with ammonium persulphate solution and were then electroplated with gold from an alkaline bath (Sel-Rex BDT-200, 5 mA cm^{-2}, 60° C) to a final deposit thickness of ~ 0.04 mm. Each through-hole was individually plated using a special fixture that allowed the bath to flow at a high rate through the hole, ensuring that deposits were reproducibly of high quality. This resulted in relatively smooth, inert, ring-shaped probes which were nearly flush with the through-hole walls, as shown by the cross-section in Fig. 2. Compared to protruding probes, the flush gold rings more closely approximate a tubular electrode and provide additional corrosion protection for the underlying copper substrate. Surface pads were individually plated under the same conditions, to a final deposit thickness of 0.06 mm.

The test board was designed to attain good spatial resolution for the larger variations in solution mass transport expected for the more important circuit board features, i.e., planes, through-holes and hole sizes. Both surface pad electrodes and through-hole probes were distributed over the surface of the board, as shown schematically in Fig. 3. The 35 circular, gold-plated pads (6 mm diameter) were arranged in seven columns with five rows each. A 1.2 mm diameter gold-plated through-hole probe was positioned 3 mm from the edge of each surface pad. Two of the pads near the board centre were surrounded by a cluster of six through-holes of diameters 0.6, 1.2, 1.6, 1.9, 2.1, and 2.4 mm, to permit determination of the effect of through-hole diameter on the amount of solution mass transport provided by a given agitation scheme. For one cluster of through-holes, the copper rings were etched ~ 0.08 mm prior to plating, so that the resultant probes were recessed

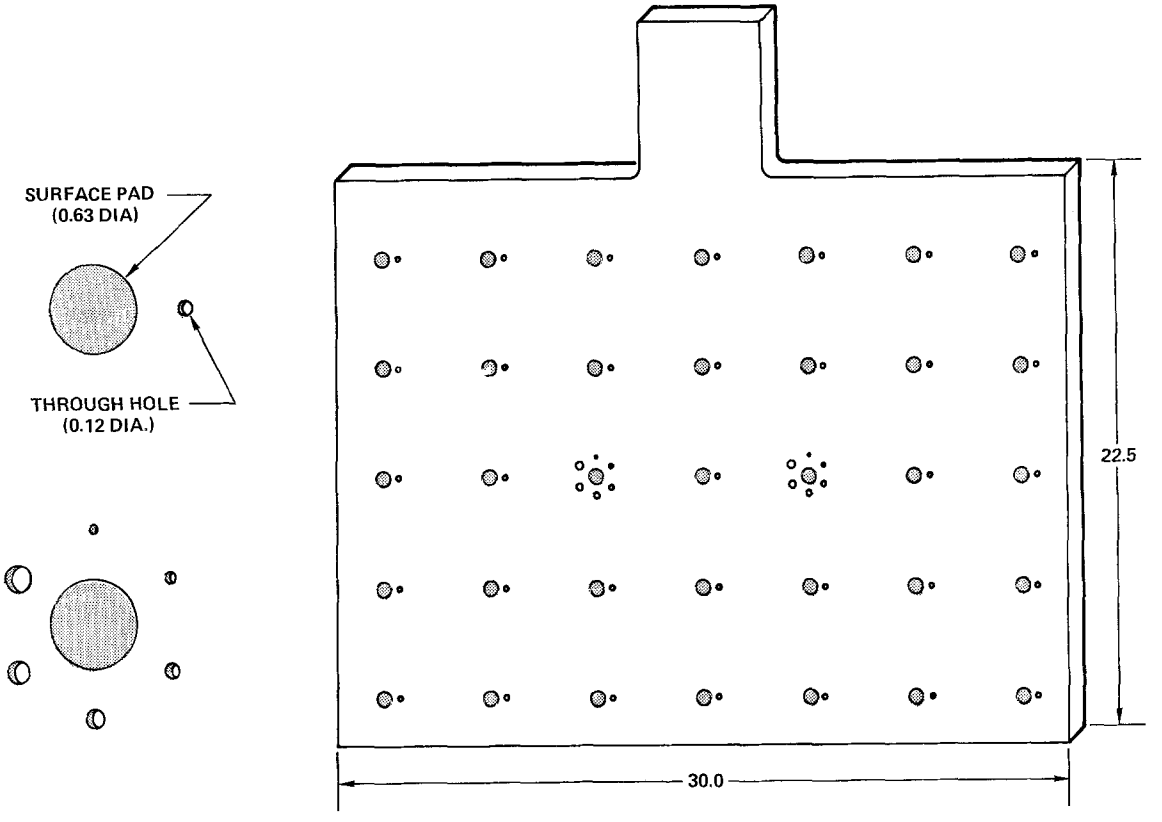

Fig. 3. Illustration of the agitation test board used in the present studies. Dimensions are in centimetres.

~ 0.04 mm relative to the epoxy–fibreglass walls, simulating the geometry of a 'positively etched-back' hole†. Pads and through-hole probes were individually connected via internal circuitry to an 80-pin terminal strip at the top of the board, thus facilitating computer-controlled data acquisition and graphic display of the results.

3.3. *Test board characterization/calibration*

Since the ferricyanide present in the test solution is sufficiently reactive to oxidize any exposed copper surfaces, cyclic voltammetry was performed in the test electrolyte for each probe after gold plating to verify its corrosion resistance. Corroding electrodes exhibit higher overall current densities, presumably because of increased surface area, and pronounced hysteresis, indicative of pitting. Probes were also tested by measuring the limiting current density as a function of time in the test electrolyte. The observed current density for typical probes was constant for test times greater than 40 hours, which represented weeks of expected use.

Each through-hole probe on the completed test board was calibrated by measuring the limiting current for ferricyanide reduction as a function of the flow rate of test electrolyte pumped through the hole. When the steady-state limiting current is plotted versus the cube root of the flow rate, a straight line is obtained, as shown for three representative probes in Fig. 4. This is in excellent agreement with hydrodynamic theory which predicts a relationship between the limiting current (i_L) and the flow rate (F) of:

$$i_L = kF^{1/3}$$

for a tubular electrode in the absence of turbulence [13], where k is a constant which depends

† Positive etchback, in which the copper circuitry layers within through-holes are recessed (by etching) relative to the laminant layers prior to plating, is a relatively common procedure used in circuit board manufacture.

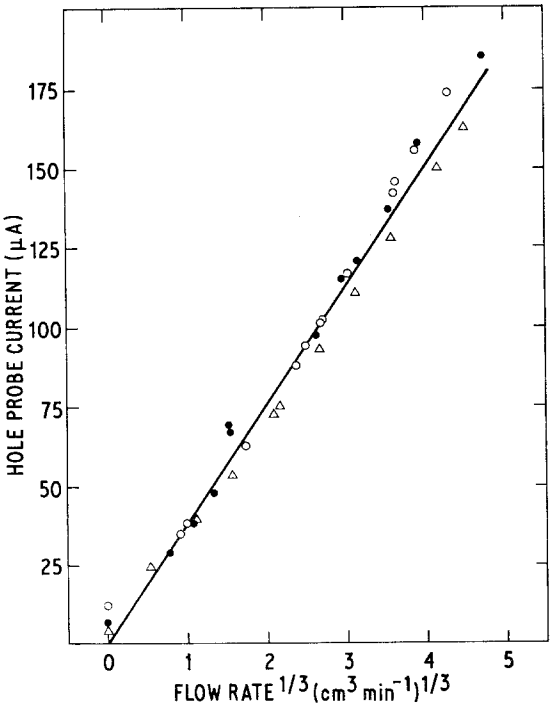

Fig. 4. Typical diffusion-limited currents for three gold through-hole probes as a function of the flow rate of 3.8 mM $Fe(CN)_6^{3-/4-}$ test electrolyte. Each symbol represents a different probe.

upon the electrode geometry, the ferricyanide concentration and the electrolyte transport properties. It should be mentioned, however, that the geometry of the through-hole probes used here, i.e., five electrically connected rings or tubes in series, is considerably more complex hydroxydynamically than a single tubular electrode. Thus, the true area of the hole probes cannot be readily ascertained from the data in Fig. 4.

3.4. *Agitation test system*

Agitation rates were measured for various combinations of air sparging and board motion in 380 dm^3 of 3.8 mmol dm^{-3} ferro–ferricyanide test electrolyte in a fibreglass tank. The electrolyte tank dimensions were 51 cm wide × 102 cm long × 73 cm deep. The test board was positioned vertically near the centre and along the length of the tank with its bottom edge submerged about 28 cm. Anodes were six platinized expanded titanium sheets, 10 cm × 10 cm × 13 cm, positioned 18 cm from the test board (three on each side). The board motion employed was back and forth (sinusoidal) at a 90° angle to the board surface at a velocity of 1.2 cm s^{-1} (2.5 cm stroke at 14 cycles min^{-1} or 0.23 cycles s^{-1}).

Air sparging was provided via 36 holes (1.6 mm diameter) in two 2.5 cm diameter (3.5 cm outside diameter) PVC pipes. The pipes were positioned symmetrically on either side of the test board, 24 cm apart, and ran parallel with the board surfaces about 8 cm from the bottom of the tank. The holes in each pipe were spaced 7.6 cm apart (centre to centre) and were arranged in two rows (of nine holes each) along the pipe axis so that the hole 'nozzles' were pointing down at a 45° angle to the vertical. This arrangement provides two relatively uniform 'sheets' of bubbles on each side of the board rising from about 8 cm below its bottom edge and extending about 16 cm past each of its ends.

Experimental control was provided by a Hewlett-Packard Model 9835 minicomputer and data were acquired via a 40-channel scanner. During experimental runs, all probes were maintained on the cathodic diffusion-limited current plateau by a power supply to ensure steady-state conditions. Probe currents were measured under potentiostatic control via a zero-impedance current follower. For each probe, the current was measured every second for 10 seconds to permit detection of local variations in electrolyte mass transport as a function of time and provide an average value to be used in evaluating the effects of other variables.

For convenience in reporting the data, we define a 'transport ratio' as the time-averaged current for a given probe with bath agitation divided by the corresponding steady-state value for that probe obtained in the bath without agitation. Through use of this dimensionless parameter, minor differences in the probe characteristics, e.g., in the surface areas, are automatically taken into account. For ascertaining the effects of agitation within through-holes, the transport ratio, which reflects the attainable current under diffusion control, is also more meaningful than electrolyte flow, on which the current has a cube root dependence [13]. For through-hole probes in the static solution, the current reaches a plateau within about 10 seconds but then continues to decay slowly, presumably because the redox species becomes depleted within the hole as the

diffusion layer thickness approaches the dimensions of the hole diameter. In this case, steady-state was taken as the beginning of the diffusion-limited plateau. Because of the uncertainty in the steady-state current for hole probes in the static electrolyte, direct comparisons of the transport ratios for hole and pad probes are not valid. Air sparging rates are reported as the volume of air flow per minute per bath surface area (m^3 min^{-1} m^{-2}).

4. Results and discussion

4.1. *Mechanical agitation only*

The sensitivity of the method is illustrated in Fig. 5 which shows typical plots of current versus time with board motion, but no gas sparging, for a 1.2 mm through-hole probe near the centre of the board. The current fluctuates sinusoidally, peaking about every two seconds as expected for back and forth motion at 0.23 cycles s^{-1} since maximum velocity of the board relative to the bath is attained twice per cycle. For through-hole probes near the edge of the board, the sine wave is not as well defined, presumably because of significant flow around the board compared to that through the holes. For surface pads near the edge of the board, the current peaks only once per cycle and the curve shape is not sinusoidal, which presumably reflects the fact that surface pads are only on one side of the board and flow occurs around the board edges. This effect is not observed for pads nearer to the centre of the board for which the currents remain relatively low and constant for board motion alone.

The uniformity of agitation provided by board motion alone is illustrated in Fig. 6, where the transport ratio (ratio of the steady-state time-averaged currents with and without bath agitation) for each probe is displayed in a three-dimensional block diagram having the test board as its base. Each block represents a probe. It is evident that mechanical board motion provides relatively high overall transport levels within through-holes (average transport ratio = 11.3) but has only a small effect on electrolyte transport to surface pads (average transport ratio = 4.4). It should be mentioned again that this comparison should not be considered absolute because of the uncertainty in the steady-state hole probe currents in the static electrolyte. As might be expected when considerable fluid flow occurs past the board edges, mass transport tends to be greatest for through-holes near the centre of the board and for surface pads near the edges.

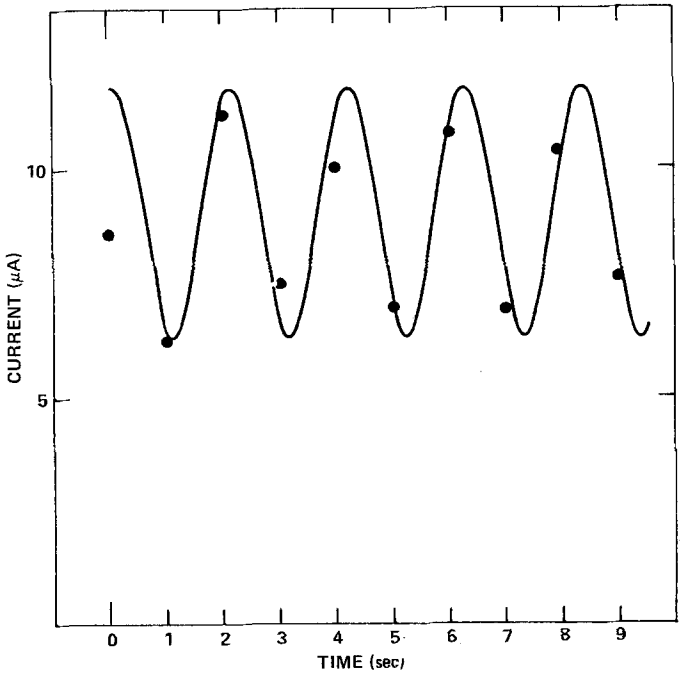

Fig. 5. Typical plot of current versus time with mechanical motion alone for a 1.2 mm through-hole probe near the centre of the board.

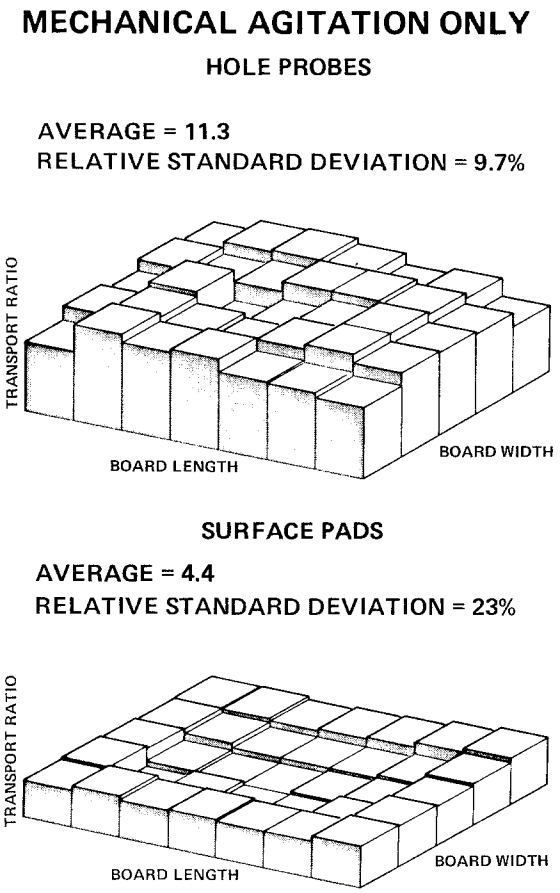

Fig. 6. Transport ratios for through-hole and surface pad probes as a function of test board position. Each block represents an individual probe.

4.2. *Mechanical agitation and air sparging*

Figs. 7 and 8 show plots of the average transport ratios for all 1.2 mm through-hole probes and all surface pads as a function of the air sparging rate, with and without board mechanical motion. It is evident that mechanical motion at low air-sparging rates provides relatively high transport levels within through-holes but has little effect on electrolyte transport to surface pads. At the higher air-sparging rates, mechanical motion has no effect on the overall transport rate for either holes or pads. Note also that for both types of probes there are two plateaus in the transport level provided by air sparging, at intermediate and high air flow rates. A thorough hydrodynamic evaluation of these features is a formidable problem which is beyond the scope of this work, but some speculation is in order. The first plateau may correspond to a transition from ordered to turbulent bubbling from the air sparger, while the second plateau could represent the practical limit of mass transport attainable with this particular agitation geometry.

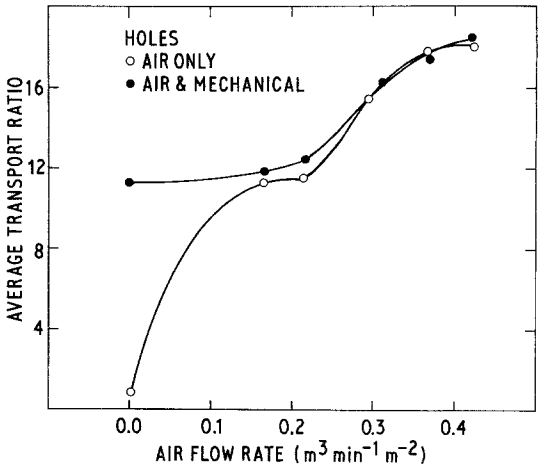

Fig. 7. Average electrolyte transport ratio versus air-sparging rate for all 1.2 mm hole probes, with and without board motion.

The value of board mechanical motion can be seen in Fig. 9 where the relative standard deviation for the time-averaged transport ratios for all 1.2 mm hole probes is plotted as a function of air-sparging rate, with and without board motion. The back and forth movement of the board is seen to significantly improve the uniformity of agitation provided by air sparging at the higher flow rates.

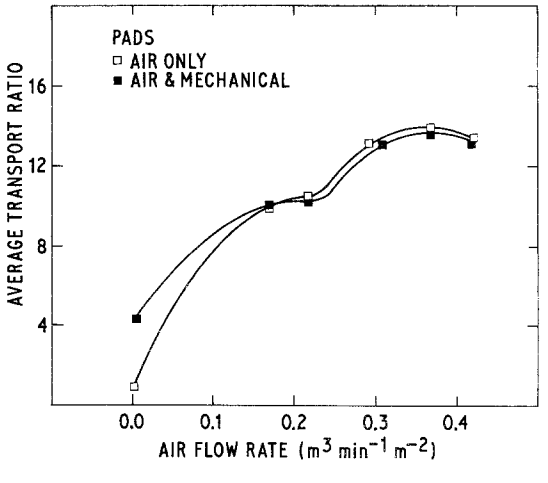

Fig. 8. Same as Fig. 7, for surface pad probes.

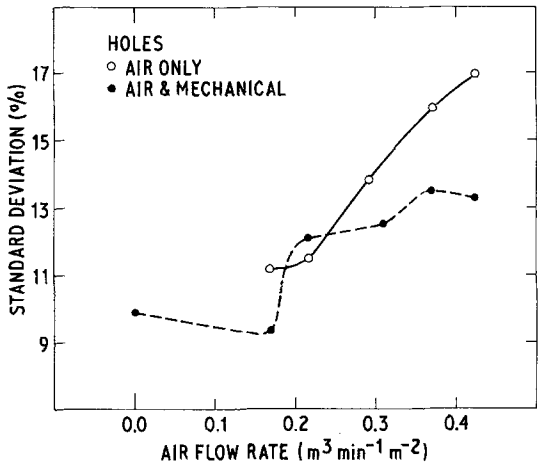

Fig. 9. Average relative standard deviation over the board surface of time-averaged transport ratios for all 1.2 mm hole probes versus air-sparging rate, with and without board motion.

Similar plots are given for surface pads in Fig. 10. In this case, board motion is detrimental to the electrolyte flow uniformity at air flow rates below 0.25 m^3 min^{-1} m^{-2}, but is beneficial at higher air-sparging rates. Note the pronounced peaks in the relative standard deviation at about 0.2 m^3 min^{-1} m^{-2} which correspond to the first plateau in the transport ratio (Fig. 8).

As shown in Fig. 11, overall electrolyte transport provided by gas sparging is significantly reduced within positively etched-back regions of the through-holes. The electrolyte transport rate also goes through minima, which averaged over many holes yield plateaus (Figs. 7 and 8) with the

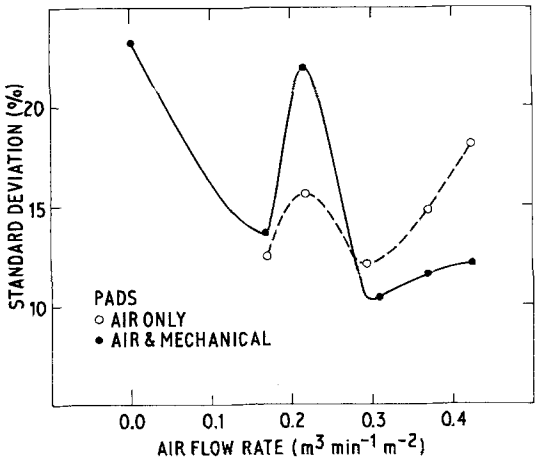

Fig. 10. Same as Fig. 9, for surface pad probes.

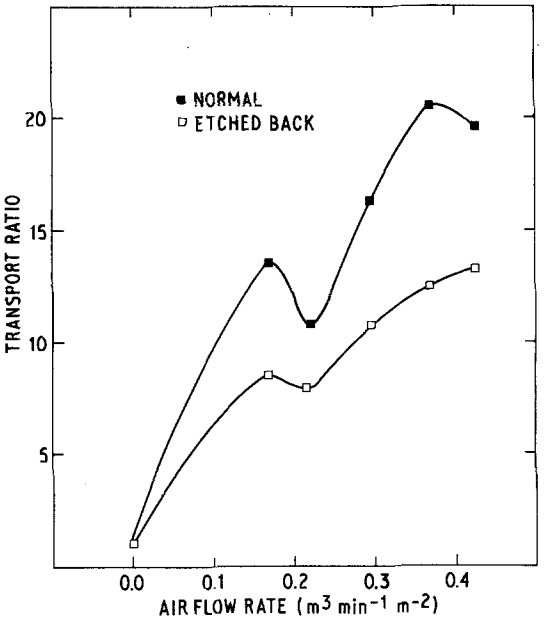

Fig. 11. Electrolyte transport ratios for a normal and an adjacent, positively etched-back 1.2 mm hole versus air-sparging rate, without board motion.

air flow rate. Fig. 12 illustrates the effect of hole diameter, for both normal and etched-back holes, on the mass transport provided by air sparging, with and without board motion. For normal holes, electrolyte mass transport increases with hole diameter up to 1.6 mm, then becomes relatively constant, going through a shallow minimum. In this case, board motion has little effect on the distribution of agitation effects among the various hole sizes. For etched-back holes, overall electrolyte mass transport is considerably lower but the effect of hole diameter is significantly less, especially with board motion. This would imply that etch-back improves the uniformity of agitation for various hole sizes, but it must be kept in mind that we are probing only the recessed portions of the holes.

Fig. 13 shows both the electrolyte flow rate within 1.2 mm through-holes and the corresponding rotation rate for a 25.4 mm diameter rotating cylinder electrode as functions of the air-sparging rate with board motion (for the agitation scheme used here). Diffusion limited currents for ferricyanide reduction at the rotating cylinder electrode were measured in the same redox electrolyte employed for the agitation studies using the electrode assembly described previously [7],

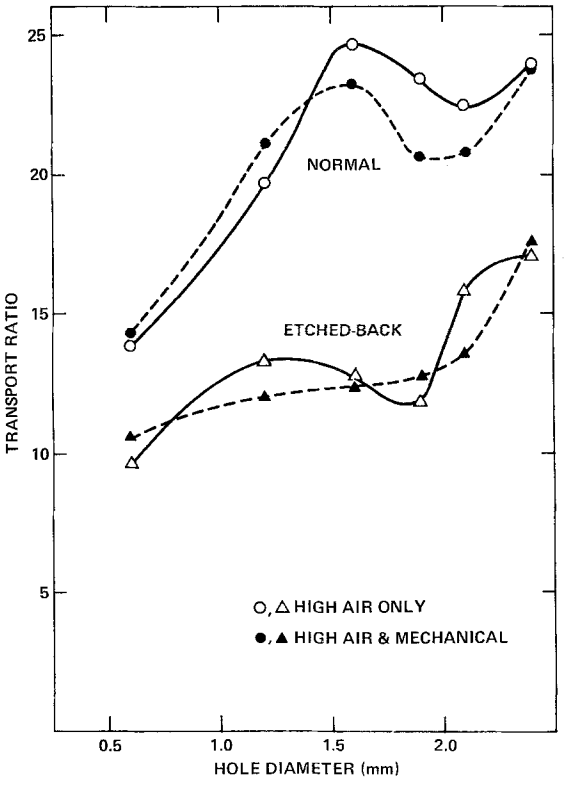

Fig. 12. Electrolyte transport ratios for normal and etched-back holes versus hole diameter for air sparging at 0.42 m^3 min^{-1} m^{-2}, with and without board motion.

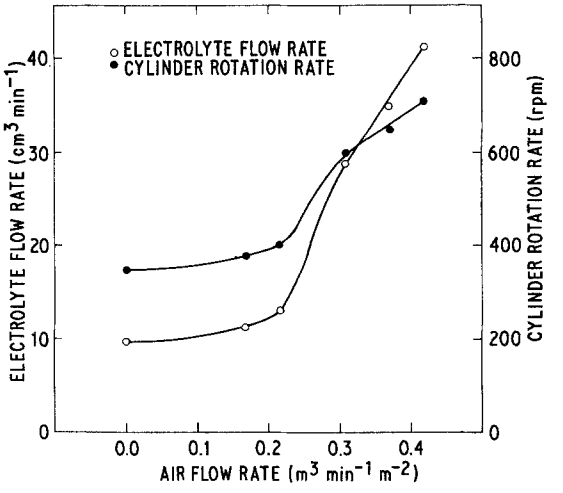

Fig. 13. Electrolyte flow rate and rotation rate for a 25.4 mm cylinder electrode versus air-sparging rate for the present agitation system with board motion.

except that the gold-plated cylinder electrode was flush with the plastic end-pieces. With plots like those in Fig. 13, laboratory data acquired using rotating electrodes can be related to the production conditions. For example, the maximum air-sparging rate (0.42 m^3 min^{-1} m^{-2}) in our agitation system produces an average electrolyte flow of about 40 cm^3 min^{-1} within 1.2 mm through-holes, which corresponds to about 700 r.p.m. for a 25.4 mm diameter cylinder. The corresponding rotation rate for a standard disc [12] electrode is about 500 r.p.m.

5. Summary and conclusions

The method described here, which involves measurement of the diffusion-limited current for a fast redox reaction at strategically located inert electrode probes, has been shown to be a sensitive means for determining the rate and uniformity of mass transport to the outer surfaces and within the through-holes of multilayer printed circuit boards. This method provides a firm basis for evaluating and improving plating-bath agitation systems, and could be applied to a variety of plating processes. An accurate knowledge of the rate and uniformity of mass transport also permits agitation effects to be taken into account in specifying process conditions.

General conclusions derived from the results obtained for a typical circuit board agitation system, involving air sparging and sinusoidal board motion perpendicular to the board surfaces, are summarized below.

(a) Mass transport rate generally increases with air-sparging rate, but two plateaus occur which should be taken into account in designing agitation systems.

(b) Uniformity of mass transport tends to decrease with increasing air-sparging rate, but the relationship is not monotonic, especially for the board outer surfaces.

(c) Perpendicular board motion has little effect on the overall mass transport rate at higher air flow rates, but significantly improves the uniformity of agitation provided by air sparging.

(d) Hole size is apparently important, i.e., mass transport is significantly restricted for diameters less than about 1.5 mm.

(e) Mass transport to positively etched-back regions within through-holes is significantly reduced.

(f) The maximum average mass transport rate

provided by the agitation scheme used in the present work corresponds to a rotation rate of about 700 r.p.m. for a 25.4 mm diameter rotating cylinder electrode [7] and about 500 r.p.m. for a standard rotating disc [12].

Acknowledgements

The authors gratefully acknowledge support of a portion of this work by the United States Air Force Materials Laboratory, Wright-Patterson Air Force Base, Ohio, under Contract No. F33615-79-C-5079. The authors are also indebted to Mr John Mather, Mr Allen Miles and Mr John Roberts for aid in performing some of the experiments.

References

[1] O. Kardos and D. Foulke, 'Advances in Electrochemistry and Electrochemical Engineering', Vol. 2, Interscience Publishers, New York (1962).
[2] D. Tench and C. Ogden, *J. Electrochem. Soc.* **125** (1978) 1218.
[3] C. Ogden and D. Tench, *Plating Surf. Finishing* **66** (1979) 30.
[4] T. Kessler and R. Alkire, *ibid* **63** (1976) 22.
[5] T. Kessler and R. Alkire, *J. Electrochem. Soc.* **123** (1976) 990.
[6] W. Engelmaier and T. Kessler, *ibid* **125** (1978) 36.
[7] C. Ogden, D. Tench and J. White, *Plating Surf. Finishing* **67** (1980) 50.
[8] R. Haak, C. Ogden and D. Tench, to be submitted to Plating Surf. Finishing.
[9] C. J. Owen, H. Jackson and E. R. York, *Plating* **54** (1967) 821.
[10] S. M. Kochergin and G. Y. Uyaseleva, 'Electrodeposition of Metals in Ultrasonic Fields', Consultants Bureau, New York (1966).
[11] ASTM D445 and D2515.
[12] V. G. Levich, 'Physicochemical Hydrodynamics', Prentice-Hall, Englewood Cliffs, N.J. (1962).
[13] R. Adams, 'Electrochemistry at Solid Electrodes', Marcel Dekker, New York (1969).